



Original Article

Virtual test occlusion for assessing ischemic tolerance using computational fluid dynamics

Tomoyoshi Kuribara¹, Takeshi Mikami¹, Satoshi Iihoshi², Toru Hirano³, Daisuke Sasamori⁴, Tadashi Nonaka⁵, Nobuhiro Mikuni¹

¹Department of Neurosurgery, Sapporo Medical University, Sapporo, Hokkaido, Japan, ²Department of Endovascular Neurosurgery, Saitama Medical University, International Medical Center, Hidaka, Saitama, Japan, ³Division of Radiology, Sapporo Medical University Hospital, Sapporo, Hokkaido, Japan, ⁴Division of Radiology, Sapporo Shiroishi Memorial Hospital, Sapporo, Hokkaido, Japan, ⁵Department of Neurosurgery, Sapporo Shiroishi Memorial Hospital, Sapporo, Hokkaido, Japan.

E-mail: *Tomoyoshi Kuribara - kuribara@sapmed.ac.jp; Takeshi Mikami - tmikami@sapmed.ac.jp; Satoshi Iihoshi - isatoshi10@gmail.com; Toru Hirano - hiranot@sapmed.ac.jp; Daisuke Sasamori - dai-sasamori@ssn-hp.jp; Tadashi Nonaka - tnonaka@ssn-hp.jp; Nobuhiro Mikuni - mikunin@sapmed.ac.jp

*Corresponding author:

Tomoyoshi Kuribara,
Department of Neurosurgery,
Sapporo Medical University,
Sapporo, Hokkaido, Japan.

kuribara@sapmed.ac.jp

Received : 02 May 2021

Accepted : 14 May 2021

Published : 27 July 2021

DOI

10.25259/SNI_439_2021

Quick Response Code:



ABSTRACT

Background: Ischemic tolerance has been evaluated by the balloon test occlusion (BTO) for cerebral aneurysms and tumors that might require parent artery occlusion during surgery. However, because of its invasiveness, a non-invasive evaluation method is needed. In this study, we assessed the possibility of virtual test occlusion using computational fluid dynamics (CFD) as a non-invasive alternative to BTO for evaluating ischemic tolerance.

Methods: Twenty-one patients who underwent BTO were included in the study. Virtual test occlusion was performed using CFD analysis, and the flow rate (FR) and wall shear stress (WSS) of the middle cerebral artery on the occlusion side were calculated. The correlations between these parameters and examination data including the parameters of computed tomography perfusion during BTO were assessed and the cutoff value of CFD parameters for detecting the good collateral group was calculated.

Results: The FR was strongly correlated with mean transit time (MTT) during BTO and moderately correlated with collateral flow grade based on angiographic appearance. The WSS was moderately correlated with collateral flow grade, mean stump pressure (MSP), and MTT. Furthermore, the FR and WSS were strongly correlated with the total FR and the diameters of the inlet vessels. The cutoff value of FR for detecting the good collateral group was 126.2 mL/min, while that of the WSS was 4.54 Pa.

Conclusion: The parameters obtained through CFD analysis were correlated with collateral flow grade and MSP in addition to MTT. CFD analysis may be useful to evaluate ischemic tolerance as a non-invasive alternative to BTO.

Keywords: Balloon test occlusion, Computational fluid dynamics, Computed tomography perfusion, Flow rate, Wall share stress

INTRODUCTION

Ischemic tolerance has been evaluated by balloon test occlusion (BTO) for large and giant cerebral aneurysms^[6,16] and head and neck tumors^[2,23] that might require parent artery occlusion during surgery. Using BTO, the risk of acute ischemic stroke can be evaluated to observe symptom progression during temporary occlusion of the parent artery as the internal carotid artery (ICA) or vertebral artery (VA) since the first report of its use in 1974.^[25] A previous review showed that the ischemic stroke rate for abrupt ICA occlusion was 26% without BTO versus

This is an open-access article distributed under the terms of the Creative Commons Attribution-Non Commercial-Share Alike 4.0 License, which allows others to remix, tweak, and build upon the work non-commercially, as long as the author is credited and the new creations are licensed under the identical terms.

©2021 Published by Scientific Scholar on behalf of Surgical Neurology International

13% with BTO.^[18] The risk of delayed ischemic stroke has also been assessed by various objective parameters including angiographic appearance, stump pressure, near-infrared spectroscopy cerebral oximeter, xenon-enhanced computed tomography (CT), single-photon emission CT, positron emission tomography, and digital subtraction angiography (DSA) equipment during BTO.^[1,3,5,11,18,22,31,32,34-36] However, the complication rate of this procedure was reportedly 3.7% in 300 cases,^[33] and its invasiveness cannot be ignored. Therefore, a non-invasive alternative to BTO is needed.

Image-based computational fluid dynamics (CFD) are able to extract patient-specific hemodynamic information based on the imaging data obtained through CT angiography (CTA), 3-dimensional (3D) DSA, and magnetic resonance angiography.^[10,27,28] Their utilities have been reported in cerebral aneurysm, atherosclerotic lesion, moyamoya disease, trigeminal neuralgia, and hemifacial spasm.^[9,12,13,24,27,29,30,37,38] Only one study to date have evaluated ischemic tolerance using image-based CFD as an alternative to BTO,^[4] and the correlation between flow rate (FR) obtained through CFD and cerebral blood flow (CBF) on ¹²³I-IMP single-photon emission CT during BTO has been revealed. In this study, BTO has been performed with CT perfusion, stump pressure, and near-infrared spectroscopy cerebral oximeter *in vivo* optical spectroscopy (INVOS) (Nihon Kohden Corp., Tokyo, Japan) examinations in addition to the conventional neurological examination and collateral angiography. Then, we evaluated possibility of virtual test occlusion using CFD analysis versus BTO, comparing the parameters obtained through virtual test occlusion with several modalities during BTO.

MATERIALS AND METHODS

Patients

The study protocol was approved by the ethics committee of Sapporo Medical University Hospital. As this study had a retrospective design, patient consent was obtained with an opt-out policy using a website. From March 2015 to February 2020, consecutive patients who underwent BTO of the ICA at our hospital were enrolled in the study. The patients were diagnosed with cerebral aneurysms, head and neck tumors, and other conditions (intracranial infection) that might require parent artery occlusion during surgery. Patients under 10-years-old and those who required BTO of other arteries were excluded from the study. A total of 21 patients (seven males and 14 females) were examined. The median age (interquartile range) of the patients was 61.0 (50.0–69.5) years (range, 11–74 years). The diagnoses of the 21 patients included cerebral aneurysm in four; head and neck tumor in 15; and other in two.

BTO

All procedures were performed using single-plane DSA equipment (Infinix Celeve-i INFX-8000C, Canon Inc., Tokyo, Japan) as previously described.^[14] The clinical, stump pressure, and INVOS examinations were performed in addition to collateral angiography during the temporal occlusion. Following collateral angiography, keeping the balloons inflated, CT perfusion was performed with interventional radiology CT equipment without patient room-to-room transfer. If the patients presented with ischemic symptoms during the occlusion, the balloons were deflated immediately regardless of the collateral angiography or CT perfusion. The appearance on collateral angiography was divided into five grades (0–4) based on the collateral flow grading system defined by the American Society of Intervention and Therapeutic Neuroradiology/Society of Interventional Radiology.^[8] This scale was designed for stroke recanalization. We modified this scale and evaluated the collateral angiographic appearance during BTO as previously described.^[14] The Grade 4 group was defined as the good collateral group with rapid collateral flow (within 2 s of the contralateral side), while the groups with Grade 3 or less were defined as the poor collateral group with slow collateral flow (more than 2 s slower than the contralateral side). Patients who could not undergo collateral angiography because of ischemic symptoms during temporal occlusion were classified into the poor collateral group.

Stump pressure was measured using a 3.3-Fr MASAMUNE balloon catheter (Fuji Systems Corp., Tokyo, Japan) placed in the ICA on the lesion side. The ratio of the mean stump pressure (MSP) before and after the temporal occlusion adjusted by mean blood pressure taken from a cuff on the left upper arm was calculated as MSP_{BR} ($[MSP\ 10\ min\ after\ occlusion/mean\ blood\ pressure\ 10\ min\ after\ occlusion]/[MSP\ before\ occlusion/mean\ blood\ pressure\ before\ occlusion]$) (BR; ratio before and after temporal occlusion).

The INVOS examination was performed during the temporary occlusion. The ratio of INVOS before versus after the temporal occlusion adjusted by INVOS on the contralateral side was calculated as $INVOS_{BR}$ ($[INVOS\ on\ the\ lesion\ side\ 10\ min\ after\ the\ occlusion/INVOS\ on\ the\ contralateral\ side\ 10\ min\ after\ the\ occlusion]/[INVOS\ on\ the\ lesion\ side\ before\ the\ occlusion/INVOS\ on\ the\ contralateral\ side\ before\ the\ occlusion]$).

If the temporary occlusion was <10 min due to ischemic symptoms, MSP and INVOS values just before balloon deflation were used.

CT perfusion during BTO

CT perfusion was performed using interventional radiology CT equipment with 16 rows (Aquilion 16 LB; Canon Inc.).

The CT perfusion scanning parameters were described previously.^[14] The CT perfusion information was transferred to a workstation (ZIOSTATION 2; Ziosoft Inc., Tokyo, Japan), and 3D multicolored images were produced. Standard single-value decomposition was implemented for the deconvolution algorithm. A region of interest (ROI) showing arterial input function was manually applied at a single branch of an insular segment of the middle cerebral artery (MCA) in the unimpaired hemisphere. A ROI showing the venous output function was also established on the superior sagittal sinus. The CBF (mL/100 g/min) in the MCA territory on the lesion and contralateral sides was measured by the manual creation of an ROI over this area along the level of the basal ganglia. The asymmetry ratio (AR) of the CBF was then calculated as $CBF_{AR} = ([CBF \text{ on the lesion}] / [CBF \text{ on the contralateral side}]) \times 100 (\%)$. Similarly, the cerebral blood volume (CBV) (mL/100 g), mean transit time (MTT) (seconds), and time to peak (TTP) (seconds) were measured, and their AR was calculated as $CBV_{AR} = ([CBV \text{ on the lesion side}] / [CBV \text{ on the contralateral side}]) \times 100 (\%)$; $MTT_{AR} = ([MTT \text{ on the lesion side}] / [MTT \text{ on the contralateral side}] - 1) \times 100 (\%)$; $TTP_{AR} = ([TTP \text{ on the lesion side}] / [TTP \text{ on the contralateral side}] - 1) \times 100 (\%)$.

Virtual test occlusion based on CFD analysis

The CTA examination was performed before BTO using a multidetector-row CT scanner with 320 rows (Aquilion ONE; Canon Inc.). The 3D-CTA scanning parameters were as previously described.^[7] The CTA information was transferred to a workstation (ZIOSTATION 2). The 3D images that included bilateral ICA (from the petrous portion), MCA (the first segment: M1), anterior cerebral artery (the first and second segments: A1 and A2, respectively), VA (from the intradural portion), basilar artery, posterior cerebral artery (the first and second segments: P1 and P2, respectively), posterior communicating artery (PcomA), and anterior communicating artery (AcomA) were produced at a threshold of 30% based on the CT value of M1 on the lesion side by a volume-rendering algorithm [Figure 1a]. The ophthalmic, superior cerebellar, anterior inferior cerebellar, and posterior inferior cerebellar arteries and other small branches were excluded in the image processing. In cases of vessel adhesion, manual processing was performed, especially in bilateral A2.

In ZIOSTATION 2, the 3D image data were transformed to stereolithography (STL) format and Hemoscope Ver.1.5 (EBM Corp., Tokyo, Japan) was used for further image processing and analysis. In the vessel module, extraction of the center lines, segmentation, and labeling of the associating vessels (bilateral ICA, M1, A1, A2, VA, P1, P2, PcomA) were performed. These vascular geometries were filled with unstructured cells mainly consisting of hexahedrons approximately 0.25 mm in the far-wall regions and 0.125 mm

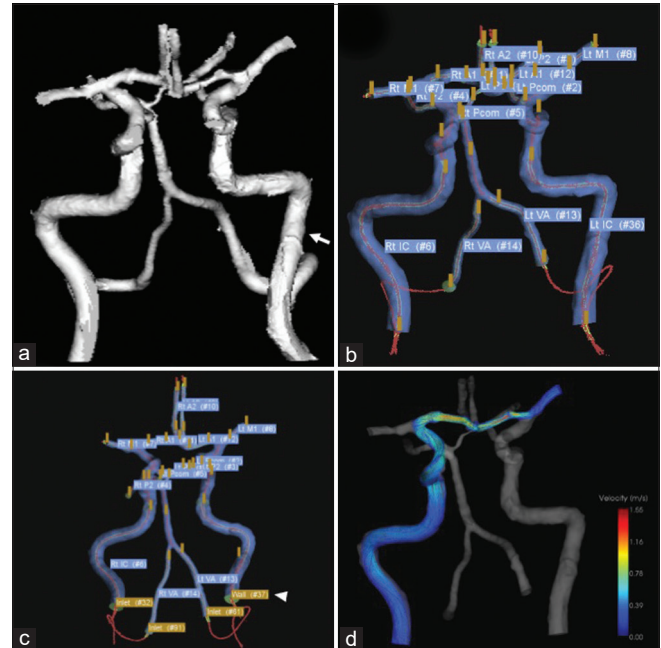


Figure 1 : A case of left middle fossa tumor. Three-dimensional imaging data were obtained through CTA using a volume-rendering algorithm. (a) The white arrow shows the ICA on the lesion side. Extraction of the center lines and segmentation and labeling of the associated vessels were performed (b). ICA on the lesion side was set as a wall (white arrowhead), while that of the contralateral ICA and bilateral VA were set as the inlet, and the on-site analysis was run (c). After the analysis, the stream line contributing to M1 on the lesion side is shown (d). CTA: Computed tomography angiography, ICA: Internal carotid artery, M1: First segment of the middle cerebral artery, VA: vertebral artery.

(width) and 0.05 mm (height) in the near-wall regions. In the near-wall regions, the meshes were aligned to fit the boundary with three layers. The inlet (contralateral ICA, bilateral VA) and outlet vessels (bilateral M1, A2, P2) were extended as long as possible based on imaging data and trimmed their proximal and distal ends [Figure 1b]. Then, an automatic measurement was performed to confirm the anatomical information of the associated vessels. In the validated CFD module, the ICA on the lesion side was set as the wall, while that of the contralateral ICA and bilateral VA were set as the inlet and the on-site analysis was run [Figure 1c]. The boundary conditions were determined according to a constant WSS theory (1.5 Pa). Specifically, FR of the inlet and outlet vessels was calculated using the Hagen-Poiseuille equation:

$$Q = \frac{\tau\pi}{32\mu} D^3 \quad (1)$$

where Q, τ , μ , and D denote FR (mL/min), WSS (Pa), fluid viscosity, and vascular diameter, respectively. After total FR at the inflow vessels was calculated, the amount of FR was

distributed at each outlet vessel according to equation;^[1] the specified boundary conditions of the inlet and outlet vessels were the pressure and velocity boundary conditions, respectively. The present computation adopted a steady flow, and the inlet pressure was set at 100 mmHg.

CFD analysis was performed using a finite volume method to solve the 3D unsteady Navier-Stokes equations and equation of continuity. Blood was assumed to be an incompressible and Newtonian fluid with a density of 1050 kg/m³ and a viscosity of 0.004 Pa s. The Euler and second-order upwind schemes were utilized to discern unsteady and convective acceleration terms. The convergent criteria were set to 10⁻⁴. Mean FR (mL/min) and mean WSS of the target vessels was obtained thorough this analysis, and the values (FR and WSS of M1 on the lesion side and FR of all inlet vessels) were evaluated. We named this simulation method virtual test occlusion. This method included vessels that were associated with perfusion on the lesion side. The virtual test occlusion with a steam line contributing to M1 on the lesion side is shown in [Figure 1d]. In case neither the AcomA nor the PcomA was sufficient for the CFD analysis, we defined their FR and WSS of M1 on the lesion side and FR of all inlet vessels as 0.

Statistical analysis

The data are expressed as median (interquartile range). Spearman's rank correlation coefficient was used to confirm the correlation between the parameters of virtual test occlusion and those of other modalities. A correlation coefficient (ρ) larger than 0.7, between 0.4 and 0.7, and between 0.2 and 0.4 indicated strong, moderate, and weak correlations, respectively. Receiver operating characteristic (ROC) curve analysis was used to determine the most suitable cutoff value of FR and WSS to detect good collateral groups based on the shortest distance from the curve to the upper left corner. Statistical analyses were performed using SPSS software (version 25; IBM Corporation, Armonk, NY, USA). $P < 0.05$ was considered statistically significant.

RESULTS

Correlations between parameters of virtual test occlusion and those of other modalities

Patient characteristics are shown in Table 1. Collateral angiography, CT perfusion, stump pressure, and INVOS examinations were successfully performed in 19, 11, 17, and 18 patients, respectively. The main reasons for not performing these examinations were presentation of ischemic symptoms during the test occlusion in five patients and insufficient room and device setting in the remaining patients. The median diameter of the ICA and M1 on the lesion side, contralateral ICA, and bilateral VA and the

total diameter of the inlet vessels included in the virtual test occlusion were 5.4 mm (5.0–5.9 mm), 3.1 mm (2.9–3.4 mm), 5.3 mm (4.6–6.0 mm), 3.2 mm (2.7–3.6 mm), and 11.2 mm (8.9–12.6 mm), respectively. The median FR, WSS of M1 on the lesion side, and FR of all inlet vessels were 80.4 mL/min (0.0–151.6 mL/min), 3.4 Pa (0.0–5.9 Pa), and 317.0 mL/min (0–574.6 mL/min), respectively. The distribution of collateral flow grade was as follows: Grade 0, 1 = 0; Grade 2 = 4; Grade 3 = 9; and Grade 4 = 6. The median CBF_{AR}, CBV_{AR}, MTT_{AR}, TTP_{AR}, MSP_{BR}, and INVOS_{BR} were 95.0% (79.5–96.5%), 106.9% (101.1–110.7%), 10.5% (8.0–37.0%), 3.6% (0.2–19.1%), 50.9% (31.2–65.2%), and 98.4% (92.0–101.1%), respectively.

A summary of the correlations is shown in Table 2. Compared with the parameters obtained during BTO, FR of M1 on the lesion side showed a strong correlation with MTT_{AR} ($\rho = -0.784$, $P = 0.004$); moderate correlations with collateral flow grade ($\rho = 0.684$, $P = 0.001$), CBF_{AR} ($\rho = 0.482$, $P = 0.133$), and MSP_{BR} ($\rho = 0.447$, $P = 0.072$); and a weak correlation with TTP_{AR} ($\rho = -0.333$, $P = 0.318$) with the exception of CBV_{AR} ($\rho = 0.145$, $P = 0.670$) and INVOS_{BR} ($\rho = 0.079$, $P = 0.756$). WSS of M1 on the lesion side showed moderate correlations with collateral flow grade ($\rho = 0.647$, $P = 0.003$), MTT_{AR} ($\rho = -0.697$, $P = 0.017$), TTP_{AR} ($\rho = -0.528$, $P = 0.095$), and MSP_{BR} ($\rho = 0.571$, $P = 0.017$), and a weak correlation with CBV_{AR} ($\rho = -0.245$, $P = 0.467$) with the exception of CBF_{AR} ($\rho = 0.173$, $P = 0.612$), and INVOS_{BR} ($\rho = -0.043$, $P = 0.865$). In the parameters obtained during BTO, MTT_{AR} was most strongly correlated with FR and WSS of M1 on the lesion side. Scatter diagrams showing the notable correlations are shown in [Figure 2]. FR was significantly correlated with collateral flow grade and MTT_{AR}, and WSS

Table 1: Patient characteristics.

Patients, N	21
Age, y, median (IQR)	61.0 (50.0–69.5)
Sex, male/female	7/14
Disease subtype, vascular/tumor/other	4/15/2
Side, rt./lt.	10/11
Diameter of ICA on the lesion side, mm, median (IQR)	5.4 (5.0–5.9)
Diameter of M1 on the lesion side, mm, median (IQR)	3.1 (2.9–3.4)
Diameter of contralateral ICA, mm, median (IQR)*	5.3 (4.6–6.0)
Mean diameter of bilateral VA, mm, median (IQR)*	3.2 (2.7–3.6)
Total diameter of inlet vessels, mm, median (IQR)*	11.2 (8.9–12.6)

ICA: Internal carotid artery, IQR: Interquartile range, Lt: left, M1: The first segment of the middle cerebral artery, Rt: Right, VA: Vertebral artery. *Including vessels associated with perfusion on the lesion side in the computational fluid dynamics analysis.

Table 2: Correlations between parameters of CFD analysis and those other modalities during BTO.

	FR (mL/min)		WSS (Pa)	
	Spearman's ρ	P value	Spearman's ρ	P value
CFG	0.684	0.001*	0.647	0.003*
CBF _{AR} , %	0.482	0.133	0.173	0.612
CBV _{AR} , %	0.145	0.670	-0.245	0.467
MTT _{AR} , %	-0.784	0.004*	-0.697	0.017*
TTP _{AR} , %	20.333	0.318	-0.528	0.095
MSP _{BR} , %	0.447	0.072	0.571	0.017*
INVOS _{BR} , %	0.079	0.756	-0.043	0.865
Diameter of ICA on the lesion side, mm	0.648	0.012*	0.358	0.208
Diameter of M1 on the lesion side, mm	0.556	0.039*	0.059	0.840
Diameter of contralateral ICA, mm**	0.709	0.007*	0.626	0.022*
Mean diameter of bilateral VA, mm**	0.567	0.054	0.354	0.259
Total diameters of inlet vessels, mm**	0.886	<0.001*	0.833	<0.001*
Total FR of inlet vessels, mL/min**	0.962	<0.001*	0.957	<0.001*

BTO: Balloon test occlusion, CBF: Cerebral blood flow, CBV: Cerebral blood volume, CFD: Computational fluid dynamics, CFG: Collateral flow grade, FR: Flow rate, ICA: Internal carotid artery, INVOS: *In vivo* optical spectroscopy, M1: The first segment of middle cerebral artery, MSP: Mean stump pressure, MTT: Mean transit time, TTP: Time to peak, VA: Vertebral artery, WSS: Wall shear stress. *Indicating statistical significance, **Including vessels associated with perfusion on the lesion side in the CFD analysis.

was significantly correlated with collateral flow grade, MTT_{AR}, and MSP_{BR} in the parameters obtained through BTO.

We subsequently evaluated the anatomical factors that affect the parameters of M1 on the lesion side obtained through virtual test occlusion. The FR of M1 on the lesion side showed strong correlations with the diameter of the contralateral ICA ($\rho = 0.709$, $P = 0.007$), total diameter of the inlet vessels ($\rho = 0.886$, $P < 0.001$), and total FR of the inlet vessels ($\rho = 0.962$, $P < 0.001$) and moderate correlations with ICA diameter on the lesion side ($\rho = 0.648$, $P = 0.012$), diameter of M1 on the lesion side ($\rho = 0.556$, $P = 0.039$), and mean diameter of the bilateral VA ($\rho = 0.567$, $P = 0.054$).

WSS of M1 on the lesion side showed strong correlations with total diameter of the inlet vessels ($\rho = 0.833$, $P < 0.001$) and total FR of the inlet vessels ($\rho = 0.957$, $P < 0.001$) and a moderate correlation with contralateral ICA diameter ($\rho = 0.626$, $P = 0.022$) and weak correlations with ICA diameter on the lesion side ($\rho = 0.358$, $P = 0.208$) and mean diameter of the bilateral VA ($\rho = 0.354$, $P = 0.259$) with the exception of M1 diameter on the lesion side ($\rho = 0.059$, $P = 0.840$). Regarding anatomical factors, total FR of the inlet vessels was most strongly correlated with FR and WSS of M1 on the lesion side. It was also obtained through virtual test occlusion depending on anatomical information.

ROC curve analysis of good collateral group

The good collateral group consisted of six patients, while the poor collateral group consisted of 15 patients. The ROC curve analysis of FR and WSS of M1 on the lesion side to detect the good collateral group is shown in [Figure 3]. The most suitable cutoff value of FR obtained through ROC curve analysis was 126.2 mL/min (sensitivity: 83.3%; and specificity: 86.7%), and that of WSS was 4.54 Pa (sensitivity: 83.3%, and specificity: 86.7%).

DISCUSSION

Utility of virtual test occlusion for assessing ischemia

In this study, the CFD parameters were correlated with collateral flow grade, MSP, and MTT. Collateral angiographic appearance, stump pressure, and MTT obtained through CT perfusion during BTO are reportedly predictors of ischemic tolerance,^[1,14,34,35] and these results might indicate that the CFD parameters represent the ischemic tolerance for non-invasively detecting the risk of delayed ischemic stroke. In the previous report, Charbel *et al.* indicated a decrease in FR in both the ipsilateral M1 and A1 segments, calculated by image based CFD model, that was greater than 20% was 100% sensitive and 100% specific in identifying patients who could not tolerated the BTO.^[4] We confirmed the results also using the other parameter, WSS, in addition to FR, comparing with several modalities during BTO. To date, the utility of WSS has been reported mainly in cerebral aneurysm in that low WSS might facilitate the growing phase and trigger cerebral aneurysm rupture by causing degenerative changes in the aneurysm wall.^[27] On the other hand, FR and WSS obtained through CFD analysis reportedly reflect the actual cerebral hemodynamic condition and are useful for detecting the risk of ischemic stroke. Mori *et al.* reported low WSS and WSS gradient values of the ipsilesional lateral striate artery (LSA) compared with that of the contralateral side in patient with LSA-territory infarcts, and CFD factors of LSA could be a risk factor for LSA-territory infarctions.^[19] In patients with

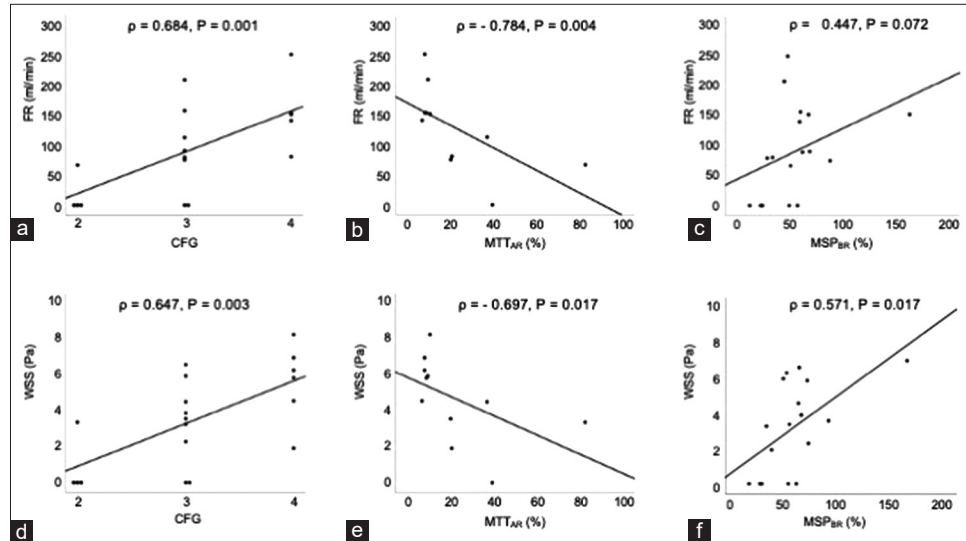


Figure 2: Scatter diagrams showing the correlations between FR and collateral flow grade (a), MTT_{AR} obtained through CT perfusion (b) and MSP_{BR} (c), WSS and collateral flow grade (d), and MTT_{AR} (e) and MSP_{BR} (f). CT: Computed tomography, FR: Flow rate; AR: Asymmetry ratio, BR: Ratio before and after temporal occlusion, MTT: Mean transit time; MSP: Mean stump pressure, WSS: Wall share stress.

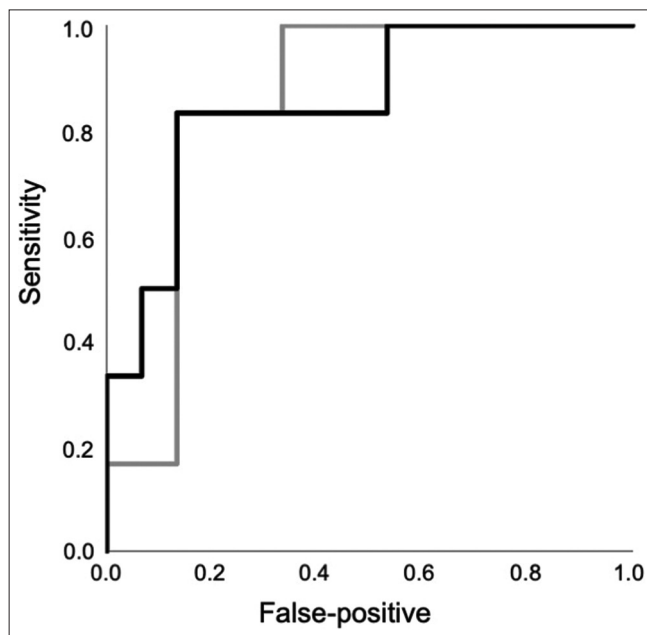


Figure 3: The gray and black lines showing a ROC curve analysis of the good collateral group detected by FR and WSS, respectively. FR: Flow rate, ROC: Receiver operating characteristic, WSS: Wall share stress.

symptomatic intracranial atherosclerotic disease, Leng *et al.* reported that translesional WSS ratio was independently associated with recurrent ischemic stroke in the same territory within 1 year.^[17] In this manner, FR and WSS obtained through CFD may be used to non-invasively detect the risk of delayed ischemic stroke.

Regarding the items influencing CFD parameters, FR and WSS might be reflected, particularly inlet vessel diameter.

FR obtained through CFD analysis reportedly reflects actual cerebral hemodynamic condition depending on anatomical structures. Kataoka *et al.* reported that vessel diameter and FR of intracranial arteries might be controlled so WSS remains constant after bypass surgery.^[12] Zhu *et al.* reported that FR, vessel diameter, and pressure decrease in ICA on the surgical side declined significantly following surgery for moyamoya disease.^[38] FR is calculated using the aforementioned equation [1] in image-based CFD analysis, primarily depending on vascular diameter. In the present study, FR of M1 on the lesion side was strongly correlated with the diameter of the contralateral ICA and the total diameters and FR of the inlet vessels. Consequently, the diameters of the associating vessels might be important for ischemic tolerance if the diameters of the AcomA or PcomA were sufficient for the CFD analysis.

Indications for recanalization with parent artery occlusion

In the present study, the most suitable cutoff values of FR and WSS for detecting the good collateral group obtained through ROC curve analysis were 126.2 mL/min and 4.54 Pa, respectively. These values represent the requirement for good collateral screening, and not indicating the need for revascularization surgery. The quantification of ischemic tolerance with FR and WSS obtained through virtual test occlusion using CFD analysis is expected to indicate ICA occlusion without high-flow bypass. However, the indications for revascularization surgery should be considered carefully with an appropriate safety margin to avoid delayed ischemic stroke. Regarding the requirement for revascularization surgery, various parameters using BTO have been reported

previously. Abud *et al.* reported that carotid sacrifice without bypass was possible when the delay between the venous drainage of the injected and occluded hemisphere was <3 s.^[1] Shimizu *et al.* reported no ischemic complications for endovascular parent artery occlusion in patients with a venous phase delay <1 s during BTO.^[26] Labeyrie *et al.* reported delayed ischemic events due to hemodynamic context for endovascular parent artery occlusion in patients who had a well-tolerated BTO with a relative delay of venous filling of <4 s were most often transient and had a good prognosis.^[15] Based on these findings, patients whose FR and WSS obtained through virtual test occlusion using CFD analysis more than 126.2 mL/min and 4.54 Pa might be treated by ICA occlusion without high-flow bypass with or without low-flow bypass, although prospective validation is needed to confirm this.

Limitations and future work

This study has several limitations. First, visualization of the small vessels such as the AcomA and PcomA was difficult because of partial volume effect and transformation to an STL format. The mean diameters of the AcomA and PcomA were reportedly 1.5 mm and 1.4–1.6 mm, respectively,^[20,21] and vessels whose diameters were <1.0 mm were difficult to detect using our method. However, these cases all showed acute ischemic symptoms or poor collateral appearances, and there was no need to detect the risk of delayed ischemic symptoms using CFD analysis. Second, the technical quality of CTA imaging could affect the result. Finally, a difference must exist between CFD and the actual hemodynamic condition because no biological information was available. Blood flow must be distributed on demand according to peripheral vascular resistance in the actual mechanisms. In addition, blood cells could not be ignored in terms of the blood flow in small vessels such as the AcomA and PcomA. Despite these limitations, our findings indicate the utility of FR and WSS obtained through virtual test occlusion using the CFD analysis method is a non-invasive alternative to BTO. It will be necessary to confirm our results with future prospective and large sample studies.

CONCLUSION

Among the parameters obtained through CFD analysis, FR and WSS were correlated with collateral flow grade and MSP in addition to MTT. The good collateral group could be distinguished using virtual test occlusion and might be treated by ICA occlusion without high-flow bypass, although prospective validation is needed to confirm this. Most researchers focus on angiographic appearance and clinical data during BTO for detecting delayed ischemic stroke after parent artery occlusion, with little research having been done on non-invasively analyzing hemodynamic mechanisms.

Virtual test occlusion might be used to evaluate ischemic tolerance as a non-invasive alternative to BTO.

Acknowledgment

I would like to thank Kei Miyata, Sangnyon Kim, Katsuya Komatsu, Yusuke Kimura, Rei Enatsu, and Yukinori Akiyama for helpful discussions.

Declaration of patient consent

The authors certify that they have obtained all appropriate patient consent.

Financial support and sponsorship

Grant support: This work was supported in part by JSPS KAKENHI grant Number 20K15933 (to T.K.).

Conflicts of interest

There are no conflicts of interest.

REFERENCES

1. Abud DG, Spelle L, Piotin M, Mounayer C, Vanzin JR, Moret J. Venous phase timing during balloon test occlusion as a criterion for permanent internal carotid artery sacrifice. *AJNR Am J Neuroradiol* 2005;26:2602-9.
2. Adams GL, Madison M, Remley K, Gapany M. Preoperative permanent balloon occlusion of internal carotid artery in patients with advanced head and neck squamous cell carcinoma. *Laryngoscope* 1999;109:460-6.
3. Brunberg JA, Frey KA, Horton JA, Deveikis JP, Ross DA, Koeppe RA. [¹⁵O]H₂O positron emission tomography determination of cerebral blood flow during balloon test occlusion of the internal carotid artery. *AJNR Am J Neuroradiol* 1994;15:725-32.
4. Charbel FT, Zhao M, Amin-Hanjani S, Hoffman W, Du X, Clark ME. A patient-specific computer model to predict outcomes of the balloon occlusion test. *J Neurosurg* 2004;101:977-88.
5. Field M, Jungreis CA, Chengelis N, Kromer H, Kirby L, Yonas H. Symptomatic cavernous sinus aneurysms: Management and outcome after carotid occlusion and selective cerebral revascularization. *AJNR Am J Neuroradiol* 2003;24:1200-7.
6. Fox AJ, Vinuela F, Pelz DM, Peerless SJ, Ferguson GG, Drake CG, *et al.* Use of detachable balloons for proximal artery occlusion in the treatment of unclippable cerebral aneurysms. *J Neurosurg* 1987;66:40-6.
7. Hashimoto A, Mikami T, Komatsu K, Noshiro S, Hirano T, Wanibuchi M, *et al.* Assessment of hemodynamic compromise using computed tomography perfusion in combination with (123)I-IMP single-photon emission computed tomography without acetazolamide challenge test. *J Stroke Cerebrovasc Dis* 2017;26:627-35.

8. Higashida RT, Furlan AJ, Roberts H, Tomsick T, Connors B, Barr J, *et al.* Trial design and reporting standards for intra-arterial cerebral thrombolysis for acute ischemic stroke. *Stroke* 2003;34:e109-37.
9. Huang Q, Xu J, Cheng J, Wang S, Wang K, Liu JM. Hemodynamic changes by flow diverters in rabbit aneurysm models: A computational fluid dynamic study based on micro-computed tomography reconstruction. *Stroke* 2013;44:1936-41.
10. Jou LD, Quick CM, Young WL, Lawton MT, Higashida R, Martin A, *et al.* Computational approach to quantifying hemodynamic forces in giant cerebral aneurysms. *AJNR Am J Neuroradiol* 2003;24:1804-10.
11. Kai Y, Hamada J, Morioka M, Yano S, Mizuno T, Kuroda J, *et al.* Treatment strategy for giant aneurysms in the cavernous portion of the internal carotid artery. *Surg Neurol* 2007;67:148-55; discussion 155.
12. Kataoka H, Makino Y, Takanishi K, Kimura Y, Takamura K, Yagi T, *et al.* Vascular responses to abrupt blood flow change after bypass surgery for complex intracranial aneurysms. *Acta Neurochir (Wien)* 2018;160:1945-53.
13. Khan MO, Arana VT, Rubbert C, Cornelius JF, Fischer I, Bostelmann R, *et al.* Association between aneurysm hemodynamics and wall enhancement on 3D vessel wall MRI. *J Neurosurg* 2021;134:565-75.
14. Kuribara T, Mikami T, Iihoshi S, Miyata K, Kim S, Kawata Y, *et al.* Ischemic tolerance evaluated by computed tomography perfusion during balloon test occlusion. *J Stroke Cerebrovasc Dis* 2020;29:104807.
15. Labeyrie MA, Lenck S, Bresson D, Desilles JP, Bisdorff A, Saint-Maurice JP, *et al.* Parent artery occlusion in large, giant, or fusiform aneurysms of the carotid siphon: Clinical and imaging results. *AJNR Am J Neuroradiol* 2015;36:140-5.
16. Larson JJ, Tew JM Jr., Tomsick TA, van Loveren HR. Treatment of aneurysms of the internal carotid artery by intravascular balloon occlusion: Long-term follow-up of 58 patients. *Neurosurgery* 1995;36:26-30; discussion 30.
17. Leng X, Lan L, Ip HL, Abrigo J, Scalzo F, Liu H, *et al.* Hemodynamics and stroke risk in intracranial atherosclerotic disease. *Ann Neurol* 2019;85:752-64.
18. Linskey ME, Jungreis CA, Yonas H, Hirsch WL Jr., Sekhar LN, Horton JA, *et al.* Stroke risk after abrupt internal carotid artery sacrifice: Accuracy of preoperative assessment with balloon test occlusion and stable xenon-enhanced CT. *AJNR Am J Neuroradiol* 1994;15:829-43.
19. Mori F, Ishida F, Natori T, Miyazawa H, Kameda H, Harada T, *et al.* Computational fluid dynamics analysis of lateral striate arteries in acute ischemic stroke using 7T high-resolution magnetic resonance angiography. *J Stroke Cerebrovasc Dis* 2019;28:104339.
20. Pedroza A, Dujovny M, Artero JC, Umansky F, Berman SK, Diaz FG, *et al.* Microanatomy of the posterior communicating artery. *Neurosurgery* 1987;20:228-35.
21. Perlmutter D, Rhoton AL Jr. Microsurgical anatomy of the anterior cerebral-anterior communicating-recurrent artery complex. *J Neurosurg* 1976;45:259-72.
22. Ryu YH, Chung TS, Lee JD, Kim DI, Suh JH, Park CY, *et al.* HMPAO SPECT to assess neurologic deficits during balloon test occlusion. *J Nucl Med* 1996;37:551-4.
23. Sanna M, Piazza P, Ditrapani G, Agarwal M. Management of the internal carotid artery in tumors of the lateral skull base: Preoperative permanent balloon occlusion without reconstruction. *Otol Neurotol* 2004;25:998-1005.
24. Satoh T, Yagi T, Onoda K, Kameda M, Sasaki T, Ichikawa T, *et al.* Hemodynamic features of offending vessels at neurovascular contact in patients with trigeminal neuralgia and hemifacial spasm. *J Neurosurg* 2019;130:1870-6.
25. Serbinenko FA. Balloon catheterization and occlusion of major cerebral vessels. *J Neurosurg* 1974;41:125-45.
26. Shimizu K, Imamura H, Mineharu Y, Adachi H, Sakai C, Tani S, *et al.* Endovascular parent-artery occlusion of large or giant unruptured internal carotid artery aneurysms. A long-term single-center experience. *J Clin Neurosci* 2017;37:73-8.
27. Shojima M, Oshima M, Takagi K, Torii R, Hayakawa M, Katada K, *et al.* Magnitude and role of wall shear stress on cerebral aneurysm: Computational fluid dynamic study of 20 middle cerebral artery aneurysms. *Stroke* 2004;35:2500-5.
28. Steinman DA, Milner JS, Norley CJ, Lownie SP, Holdsworth DW. Image-based computational simulation of flow dynamics in a giant intracranial aneurysm. *AJNR Am J Neuroradiol* 2003;24:559-66.
29. Suzuki T, Stapleton CJ, Koch MJ, Tanaka K, Fujimura S, Suzuki T, *et al.* Decreased wall shear stress at high-pressure areas predicts the rupture point in ruptured intracranial aneurysms. *J Neurosurg* 2019;132:1116-22.
30. Takao H, Murayama Y, Otsuka S, Qian Y, Mohamed A, Masuda S, *et al.* Hemodynamic differences between unruptured and ruptured intracranial aneurysms during observation. *Stroke* 2012;43:1436-9.
31. Takeda N, Fujita K, Katayama S, Tamaki N. Cerebral oximetry for the detection of cerebral ischemia during temporary carotid artery occlusion. *Neurol Med Chir (Tokyo)* 2000;40:557-62; discussion 562-3.
32. Tani S, Imamura H, Asai K, Shimizu K, Adachi H, Tokunaga S, *et al.* Comparison of practical methods in clinical sites for estimating cerebral blood flow during balloon test occlusion. *J Neurosurg* 2019;131:1430-6.
33. Tarr RW, Jungreis CA, Horton JA, Pentheny S, Sekhar LN, Sen C, *et al.* Complications of preoperative balloon test occlusion of the internal carotid arteries: Experience in 300 cases. *Skull Base Surg* 1991;1:240-4.
34. Tomura N, Omachi K, Takahashi S, Sakuma I, Otani T, Watarai J, *et al.* Comparison of technetium Tc 99m hexamethylpropyleneamine oxime single-photon emission tomograph with stump pressure during the balloon occlusion test of the internal carotid artery. *AJNR Am J Neuroradiol* 2005;26:1937-42.
35. van Rooij WJ, Sluzewski M, Slob MJ, Rinkel GJ. Predictive value of angiographic testing for tolerance to therapeutic occlusion of the carotid artery. *AJNR Am J Neuroradiol* 2005;26:175-8.
36. Vazquez-Anon V, Aymard A, Gobin YP, Casasco A, Ruffenacht D, Khayata MH, *et al.* Balloon occlusion of the internal carotid artery in 40 cases of giant intracavernous aneurysm: Technical aspects, cerebral monitoring, and results. *Neuroradiology* 1992;34:245-51.

37. Xiang J, Damiano RJ, Lin N, Snyder KV, Siddiqui AH, Levy EI, *et al.* High-fidelity virtual stenting: modeling of flow diverter deployment for hemodynamic characterization of complex intracranial aneurysms. *J Neurosurg* 2015;123:832-40.
38. Zhu F, Qian Y, Xu B, Gu Y, Karunanithi K, Zhu W, *et al.* Quantitative assessment of changes in hemodynamics of the

internal carotid artery after bypass surgery for moyamoya disease. *J Neurosurg* 2018;129:677-83.

How to cite this article: Kuribara T, Mikami T, Iihoshi S, Hirano T, Sasamori D, Nonaka T, *et al.*: Virtual test occlusion for assessing ischemic tolerance using computational fluid dynamics. *Surg Neurol Int* 2021;12:378.